Characterization of biochar-derived dissolved organic matter using UV-visible absorption and excitation-emission fluorescence spectroscopies

ARTICLE *in* CHEMOSPHERE · DECEMBER 2013

Impact Factor: 3.34 · DOI: 10.1016/j.chemosphere.2013.11.066 · Source: PubMed

3 AUTHORS:

Tyler Jamieson
Trent University
1 PUBLICATION **11** CITATIONS
SEE PROFILE

Eric PS Sager
Trent University
15 PUBLICATIONS **193** CITATIONS
SEE PROFILE

Celine Gueguen
Trent University
59 PUBLICATIONS **1,090** CITATIONS
SEE PROFILE

Chemosphere 103 (2014) 197–204

Contents lists available at ScienceDirect

Chemosphere

journal homepage: www.elsevier.com/locate/chemosphere

Characterization of biochar-derived dissolved organic matter using UV–visible absorption and excitation–emission fluorescence spectroscopies

Tyler Jamieson [a,b], Eric Sager [c], Céline Guéguen [b,*]

[a] Environmental and Resource Studies Program, Trent University, Peterborough, ON, Canada
[b] Department of Chemistry, Trent University, Peterborough, ON, Canada
[c] Sir Sanford Fleming College, Lindsay, ON, Canada

HIGHLIGHTS

- Biochars contributed different amounts of DOC in relation to production methods.
- DOM aromaticity and mean molecular weight varied amongst different biochars.
- EEM fluorescence showed distinct DOM signatures for each biochar type.
- Transformations in biochar DOM were observed over time.

ARTICLE INFO

Article history:
Received 9 October 2013
Received in revised form 24 November 2013
Accepted 26 November 2013
Available online 17 December 2013

Keywords:
Charcoal
Aromaticity
Molecular weight
Pyrolysis
PARAFAC

ABSTRACT

In recent years, biochar has become of considerable interest for a variety of environmental applications. However, the feasibility of its application is entirely dependent on its physical and chemical properties, including the characteristics of biochar-derived dissolved organic matter (DOM). The goal of this study was to assess the use of optical analysis for the purpose of characterizing biochar-derived DOM. Three different biochars (slow pyrolysis birch and maple; fast pyrolysis maple) were produced and leached in distilled water over 17 d. Samples were taken on days 3, 10, 13 and 17, filtered, and analyzed for DOC content. Samples were also subjected to optical analysis using UV–visible absorption and excitation–emission matrix (EEM) fluorescence spectroscopies. EEM fluorescence data were further analyzed using parallel factor analysis (PARAFAC). Absorbance and fluorescence results were combined and examined using principal component analysis (PCA). Significant differences in the water soluble organic carbon content were observed for all biochar types. The estimated aromaticity ($SUVA_{254}$) and mean molecular weight ($S_{275-295}$) of biochar-derived DOM were also found to differ based on biochar type. PARAFAC analysis identified three humic-like components and one protein-like component. Distinct DOM signatures were observed for each biochar type. Transformations in biochar DOM characteristics over time were also observed. The PCA showed a clear delineation in biochar types based on their optical properties. The results of this study indicate that optical analysis may provide valuable information regarding the characteristics of biochar-derived DOM.

1. Introduction

In recent years, biochar, a carbon rich substance produced from the pyrolysis of organic matter, has become of considerable interest as a soil amendment in a number of applications, including agriculture and contaminated soil remediation (Beesley et al., 2011; Spokas et al., 2012). When added to soils, biochar can serve to sequester carbon, improve water holding capacity, improve nutrient retention, and promote microbial activity (Spokas et al., 2012). Biochar also has the ability to complex organic and inorganic contaminants to its surface, reducing their mobility and bioavailability (Beesley et al., 2011). The incorporation of biochar into soils has also been observed to increase dissolved organic matter (DOM) content in pore waters (Beesley et al., 2010). This may have important implications in terms of its application potential, as DOM greatly affects the transport, fate and toxicity of metals via the formation of DOM–metal complexes (Tipping, 2002; Guéguen et al., 2004), and plays an important role in the formation of soils (Kalbitz et al., 2000). Indeed, it has been suggested that biochar-derived DOM may provide a bioavailable source of carbon for soil microbes (Deenik et al., 2010). Previous studies have also shown

* Corresponding author. Tel.: +1 (705) 748 1011.
E-mail address: celinegueguen@trentu.ca (C. Guéguen).

0045-6535/$ - see front matter © 2013 Elsevier Ltd. All rights reserved.
http://dx.doi.org/10.1016/j.chemosphere.2013.11.066

that biochar-derived DOM can mobilize metal contaminants retained in soils (Beesley et al., 2010; Uchimiya et al., 2010). In light of the potentially important role of biochar-derived DOM in determining biochar's application potential, there has been a push to further our understanding of the soluble organic fraction of biochar (Uchimiya et al., 2010, 2013; Lin et al., 2012).

It is widely accepted that individual biochars are physically and chemically unique, which largely determines their usefulness in environmental applications (Beesley et al., 2011; Spokas et al., 2012). Feedstocks are unique in terms of their physical and chemical composition, and these characteristics are further modified depending on the conditions (i.e. high treatment temperature (HTT), heating rate, and furnace residence time) used during pyrolysis (Downie et al., 2009; Kloss et al., 2012). Indeed, the soluble organic fraction of biochar has been observed to be equally as affected by feedstock and pyrolytic conditions (Gaskin et al., 2008; Deenik et al., 2010; Lin et al., 2012; Mukherjee and Zimmerman, 2013; Uchimiya et al., 2013). Presently, studies that focus on the characterization of the soluble organic fraction of biochar are limited (Lin et al., 2012; Uchimiya et al., 2013), and further investigation is warranted.

The optical properties of dissolved organic matter (DOM), particularly its absorbance and fluorescence, are typically examined for the purpose of compositional characterization (Coble, 1996; Blough and Del Vecchio, 2002; Guéguen et al., 2012). The use of UV–visible absorption spectroscopy allows for the estimation of aromaticity and mean molecular weight, using specific absorbance ($SUVA_{254}$; Weishaar et al., 2003) and spectral slope ($S_{275-295}$; Helms et al., 2008), respectively. Excitation–emission matrix (EEM) fluorescence spectroscopy (Coble, 1996) coupled with parallel factor analysis (PARAFAC; Stedmon et al., 2003; Stedmon and Bro, 2008) can be employed to resolve the dominant fluorescent DOM components based on their excitation and emission (Ex/Em) maxima (Stedmon et al., 2003; Stedmon and Markager, 2005; Fellman et al., 2008; Guéguen et al., 2012; Cuss and Guéguen, 2013). EEM fluorescence also holds an advantage over other types of analysis: it is simple to undertake; non-destructive; sensitive; rapid; and does not require any pre-treatment of samples before analysis (Andrade-Eiroa et al., 2013). However, EEM fluorescence is limited in that it only serves to provide information on the fluorescent fraction of DOM (i.e. protein and humic-like components), while leaving out other non-fluorescent fractions, such as carbohydrates and lipids. Lignin-derived organic matter has also been observed to contribute to humic-like fluorescence (Maie et al., 2007). Regardless, the use of UV–visible absorption and EEM fluorescence spectroscopies may provide useful information for the production and study of biochar. Indeed, Uchimiya et al. (2013) found considerable changes in the fluorescence characteristics in relation to feedstock and pyrolysis temperature in DOM extracted from biochar over 16 h, using base (NaOH) and hot water (80 °C) extractants.

In this study, biochar-derived DOM was characterized using UV–visble absorbtion and EEM fluorescence. This was accomplished by leaching three different biochars (slow pyrolysis birch and maple; fast pyrolyisis maple) in distilled water over 17 d, and measuring the leachate DOC content, absorption, and fluorescence to observe the evolution of the biochar-derived DOM over time. The difference in qualitative characteristics of biochar-derived DOM was further investigated using principal component analysis.

2. Methods

2.1. Biochar production

Three biochars were made from a two sawmill waste feedstocks obtained from the Haliburton Forest and Wildlife Reserve located in Haliburton, Ontario. Feedstocks consisted of fine-textured (<5 mm) yellow birch (*Betula alleghaniensis*) and sugar maple (*Acer saccharum*) wood and bark chips. Two different slow-pyrolysis biochars were made with yellow birch and sugar maple feedstocks, using a batch method in which feedstock was placed in the horizontally mounted drum kiln and heated externally using two large propane burners. The yellow birch biochar (353BS) was brought to a high temperature of 353 °C over approximately 2.75 h at a heating rate of approximately 2 °C min^{-1}. The sugar maple biochar (380MS) was brought to a high temperature of 380 °C over approximately 2.5 h at a heating rate of approximately 2.5 °C min^{-1}. The drum was continuously rotated to ensure even heating. A valve was opened to allow the venting of gasses, and then sealed once degassing subsided, to minimize the incorporation of atmospheric oxygen. Both biochars were cooled within the sealed kiln, and sealed within plastic buckets once fully cooled. A third sugar maple biochar (600MF) was made using a continuous-feed flow-through system. Before the feedstock was introduced, the kiln was externally heated to an internal temperature of approximately 600 °C. Sugar maple feedstock was then fed into the tubular reactor where it was transported across the heated surface to an internal holding area through the action of a rotating auger. Because of the relatively low reactor residence time (<20 min) and fast heating rate, this biochar was classified as a fast-pyrolysis biochar.

2.2. Leaching experiment

Biochar was placed in a furnace at 60 °C overnight to evaporate any excess moisture that may have been incorporated during storage. Ten grams of biochar were mixed into 200 ml of distilled water, sealed in acid-washed translucent plastic containers, and allowed to sit in the dark at room temperature for 17 d. A total of 16 solutions were prepared: 5 replicates for each biochar type (353BS, 380MS, 600MF), and a water-only control. Leachate samples (approx. 30 mL) were extracted from each solution on days 3, 10, 13, and 17. Samples were filtered using a pre-combusted glass fibre filter (Whatman AP40; 0.7 μm). Samples designated for dissolved organic carbon (DOC) analysis were placed in clear pre-combusted (450 °C for $\geqslant$5 h) glass bottles, while samples for UV absorbance, and fluorescence were stored in pre-combusted amber-tinted glass bottles. All apparatus were thoroughly washed with ultra-pure Milli-Q water (MQW; 18 MΩ, Millipore Corp., Bedford, Massachusetts) between samples. Before samples were filtered, a small portion was used to rinse the apparatus. The leachate pH was also recorded during every sampling (Fisher Scientific, AP71). The pH range and overall mean (±SE) for 353BS, 380MS, and 600MF was 7.04–8.30 and 7.72 ± 0.06, 7.21–7.92 and 7.69 ± 0.45, 7.35–8.08 and 7.61 ± 0.04, respectively. All samples were refrigerated at 4 °C in the dark until analysis was completed.

2.3. DOC analysis

DOC content in leachate was measured using a Shimadzu TOC-VCPH analyzer (Guéguen et al., 2012). DOC concentrations in the control ranged from 0.13 to 5.49 mg L^{-1}, with an overall mean (±SE) of 2.21 ± 1.56 mg L^{-1}. DOC concentrations observed in the control were subtracted from concentrations in leachate extracted from all biochars measured on the same day. The water soluble organic carbon (WSOC; mg g^{-1}) contents of the biochar were calculated using the following equation:

$$\mathrm{WSOC} = V \times C/M$$

where V is the volume of water (L) in each leaching container at the time of sampling, C is the DOC concentration (mg L^{-1}) in the sample, and M is the mass of biochar (g) in each leaching container.

2.4. UV–visible absorption

Absorbance was measured using a Shimadzu UV 2550 spectrophotometer within a spectrum of 250–700 nm, at 1-nm increments, using a 1-cm quartz cuvette. Blanks of MQW were used as a reference. Samples were allowed to come to room temperature before measurements were taken. Reference blanks were subtracted from the measured absorption, and the absorption coefficient a (m^{-1}) was calculated for each wavelength (λ) using the equation:

$$a_\lambda = 2.303 A_\lambda / l_L$$

where A_λ is the absorbance and l_L is the path-length of the optical cell in meters (here $l = 0.01$ m). Measurements for the control were also subtracted after subtracting blank measurements, to account for any effects caused by the leaching containers. $SUVA_{254}$ (L mg^{-1} - m^{-1}) was calculated using the equation:

$$SUVA_{254} = a_{254}/DOC$$

where a_{254} is the absorbance coefficient measured at 254 nm (m^{-1}). $SUVA_{254}$ has previously been correlated to DOM aromaticity (Weishaar et al., 2003). Spectral slope ($S_{275-295}$) was determined by fitting an exponential decay model (Sigmaplot Version 11, 2008, Systat Software, Inc.) to the absorption coefficients within the spectra 275–295 nm (Helms et al., 2008). A decrease in $S_{275-295}$ suggests an increase in molecular weight (Helms et al., 2008; Guéguen and Cuss, 2011).

2.5. EEM fluorescence and PARAFAC

Fluorescence was measured using a Fluoromax-4 Jobin Yvon spectrofluorometer, using a 1-cm quartz cuvette, across excitation wavelengths ranging from 250 to 500 nm and emission wavelengths from 300 to 600 nm, at 5-nm increments (Guéguen and Cuss, 2011). Excitation wavelengths of >250 nm were selected due to the lack of manufacturer-provided calibration below an excitation wavelength of 250 nm. In addition, biochars have been observed to contain appreciable amounts of nitrogen (Spokas et al., 2012), and nitrate can create interference at excitation wavelengths <250 nm (Cuss and Guéguen, 2012a and references therein). Samples were allowed to come to room temperature before analysis. Fluorescence measurements were made using a thermostatted cell holder set to 20 °C. If the absorbance at the lowest wavelength (i.e. 250 nm) was higher than 0.05, the samples were diluted with MQW to minimize reabsorption and inner filter effects, which allows for the maintenance of a linear relationship between fluorescence intensity and concentration. Data derived from samples were corrected for dilution after processing. MQW blanks were measured and the EEMs were subtracted from biochar leachate measurements to remove Raman scattering effects. Fluorescence intensities were corrected to the area under the MQW Raman peak (excitation 350 nm) measured on the same day (Lawaetz and Stedmon, 2009). Little variation was observed in the integral of the Raman peak (<1.7%). PARAFAC analysis was carried out using MATLAB R2010a (MathWorks) with the DOMFluor toolbox following the procedure provided by Stedmon and Bro (2008). PARAFAC was applied using 2–7 component models with non-negativity constraints, and a four-component model was split-half validated on both halves using 60 distinct EEMs (99.39% variation explained).

2.6. Statistical analysis

Statistics were accomplished using Sigmaplot (Ver. 11, 2008, Systat Software, Inc.) and R Statistical Software (Ver. 2.15.1, 2012, The R Foundation for Statistical Computing). DOC concentrations, $SUVA_{254}$, $S_{275-295}$, component loadings and percent composition were compared using a one-way ANOVA on each sampling day, and individual differences were investigated post hoc using a Tukey test. Fluctuations in leachate DOC concentration were examined using a repeated-measure ANOVA. Data that did not meet the assumptions of normality and homoscedasticity were examined using rank transformed values. PARAFAC component percent composition data were normalized using the centre-log-ratio (CLR) transformation (Pawlosky-Glahn and Egozcue, 2006). PARAFAC component loadings, and component percent composition measurements taken at the beginning and end of the leaching experiment (day 3 and day 17, respectively) were examined using paired t-tests. Data that did not meet the assumptions of normality were examined using paired Wilcoxon signed-rank tests. A principal component analysis was undertaken using $SUVA_{254}$, $S_{275-295}$, and CLR-transformed PARAFAC percent composition data. Correlations were examined using Pearson correlation, and any data found to violate the assumptions of normality were examined using Spearman's Rank.

3. Results and discussion

3.1. DOC analysis

Two outlier samples were identified (353BS3, day 3; 380MS2, day 13) that showed DOC concentrations that were approximately 3 times lower than all other measurements taken on the same day, and were consequently removed from the analysis. Fig. 1 shows the mean DOC concentrations (±SE) observed in biochar leachate over time. Mean DOC concentration values (±SE) are provided as Supplementary information (Table S1). After 3 d, leachate from 600MF showed significantly higher amounts of DOC ($p < 0.0001$) than both 353BS, and 380MS, which were not significantly different ($p > 0.05$). On day 10, a decline in DOC in the 600MF leachate was observed. The slight decline in DOC found in the 600MF leachate coupled with a slight increase in DOC concentration in the 353BS leachate resulted in a significant difference between only 600MF and 380MS ($p < 0.05$), while 353BS was found to be similar to both 600MF and 380MS. On day 13, DOC in the 353BS leachate was found to be significantly higher than 380MS ($p < 0.05$), while DOC in the 600MF leachate had further declined so that it was similar to both 353BS, and 380MS. This trend held for measurements taken on day 17. Of the three biochar leachate types, only 600MF

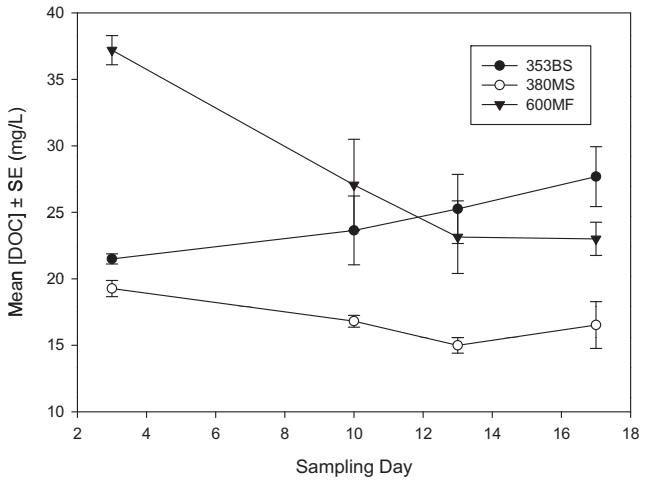

Fig. 1. Mean DOC concentrations observed in biochar leachate (±SE). Different letters indicate significant differences ($p < 0.05$) in measurements taken on the same day.

showed a significant change in DOC concentration over time ($p < 0.05$). The decrease in DOC concentration in the 600MF leachate, and the lack of significant fluctuation in DOC in the 353BS and 380MS leachates further suggests that the majority of DOC was leached from the biochars within the first 3 d of the experiment.

The estimated range and overall mean (±SE) WSOC content was 0.24–0.50 g kg^{-1} and 0.37 ± 0.02 g kg^{-1}; 0.11–0.43 g kg^{-1} and 0.27 ± 0.02 g kg^{-1}; 0.21–0.81 g kg^{-1} and 0.45 ± 0.05 g kg^{-1}, for 353BS, 380MS, and 600MF, respectively. Because of the extensive variability in feedstocks and pyrolysis procedures used to create biochar, it is difficult to compare these findings with observations made in other studies. DOC measurements taken on day 3 show a clear difference between biochars made from the same feedstock, using different pyrolytic conditions (600MF and 380MS; Fig. 1). The DOC concentration in the 600MF leachate was almost 2-fold greater than that measured in the 380MS leachate. This contrasts with other studies that found that biochars produced at low temperatures had higher DOC contents compared to biochars produced at higher temperatures (Gaskin et al., 2008; Lin et al., 2012; Mukherjee and Zimmerman, 2013). However, previous studies have also shown that biochars made using fast pyrolysis (i.e. fast heating rates and low furnace residence times) can contribute greater amounts of DOC when incorporated into soils, when compared to those made using slow pyrolysis using the same feedstock and HTT (Bruun et al., 2012). Unfortunately, because of variation in both pyrolytic conditions (i.e. HTT and heating rates) and feedstocks used to produce 353BS and 380MS, it is difficult to comment on the differences observed in their leachate DOC concentrations, as both of these factors can affect WSOC content (Gaskin et al., 2008; Deenik et al., 2010; Bruun et al., 2012; Lin et al., 2012; Mukherjee and Zimmerman, 2013). However, it was noted that by day 10 of the experiment, leachate from 353BS showed significantly higher DOC concentrations than 380MS ($p < 0.05$; Fig. 1).

The relatively fast heating rates and short furnace residence times used in fast pyrolysis can result in the incomplete pyrolysis of biomass, which in turn can result in a biochar containing a potentially bioavailable source of carbon (Bruun et al., 2012). This could account for the apparent drop in DOC concentration observed in the 600MF leachate. DOC loss can be attributed to both microbial activity, and photodegradation (Carlson, 2002). In this study, all leachate containers and DOC samples were stored in the dark, and the oldest samples showed the highest DOC concentrations, therefore DOC loss due to photodegradation is unlikely. However, it should be noted that the presence of microbial activity was not investigated; therefore, it cannot be said for certain that microbial activity is responsible for the decline in DOC observed in the 600MF leachate.

3.2. UV–visible absorption

Throughout the entire experiment, 600MF had significantly higher $SUVA_{254}$ values ($p < 0.05$; Fig. 2A), and thus the highest DOM aromaticity. Leachate from 353BS and 380MS showed similar $SUVA_{254}$ values (except at day 3; $p < 0.05$; Fig. 2A), and showed negligible change over time. Based on the linear model described by Weishaar et al. (2003), the percent of aromatic material in DOM derived from 353BS, 380MS, and 600MF could range from 8–15%, 3–13%, and 27–>50%, respectively. The increase in $SUVA_{254}$ observed in the 600MF leachate over time corresponded with the decline in DOC concentration (Figs. 1 and 2A). Fellman et al. (2008) found that $SUVA_{254}$ was negatively correlated to the more labile biodegradable fraction of DOM found in forest and wetland soils. This suggests that the decline in DOC and increase in $SUVA_{254}$ observed in the 600MF leachate could be the result of the degradation of the more labile fraction of DOC, which would increase the proportion of recalcitrant aromatics.

Mean $S_{275-295}$ values (±SE) ranged from 0.017 ± 0.001 nm^{-1} for 600MF to 0.025 ± 0.001 nm^{-1} for 353BS to 0.034 ± 0.002 nm^{-1} for 380 MS. Significant differences were found between biochars on everyday of sampling ($p < 0.05$; Fig. 2B). The WSOC mean molecular weight decreased in the order 600MF > 353BS > 380MS. Lin et al. (2012) observed a reduction in high molecular weight water extractable carbon fractions (biopolymers, building blocks, humics) and an increase in the lower molecular weight acids fractions in biochars produced at higher temperatures. This further supports the idea that 600MF may be underpyrolyzed compared to 380MS. It was also noted that low $S_{275-295}$ were associated with high $SUVA_{254}$, which is consistent with previous studies (Blough and Del Vecchio, 2002; Guéguen et al., 2012).

3.3. EEM fluorescence and PARAFAC

In the four component PARAFAC model, three components (C1–C2, C4) were classified as humic-like, and one as protein-like (C3). Contour plots of each component are provided in Fig. 3. Contour plots of fluorescence measurements from each biohcar type taken on day 3 are provided as Supplementary information (Fig. S1). C1 had primary excitation maximum at <250 nm and a secondary peak at 280 nm, with an emission maximum at 390 nm. This was labelled as a marine/microbial humic-like peak (A + M; Coble, 1996). Similar peaks have been observed in DOM in natural waters, leaf leachate (Stedmon and Markager, 2005; Ishii and Boyer, 2012; Cuss and Guéguen, 2013). Fluorophores showing peaks similar to C1 are often associated with biological activity, and are thought to be produced through the process of biodegradation (Ishii and Boyer, 2012). C2 had a primary excitation maximum of 250 nm, a secondary peak at 320 nm, and an emission maximum of 435 nm (A + C; Coble, 1996). This peak has been found ubiquitously in natural waters, and has been associated with both autochthonous and allochthonous sources (Stedmon and Markager, 2005; Ishii and Boyer, 2012; Cuss and Guéguen, 2013). Peaks similar to C1 and C2 have also been observed in biochar extracts, and were characterized as pyrolysis products consisting of (poly)phenolics and other aromatic structures similar to soil fulvic-like substances, and aromatic humic-like substances with that were observed to decompose at higher pyrolysis temperatures, respectively (Uchimiya et al., 2013). C4 had a primary excitation maximum of 350 nm, a secondary excitation maximum of 290 nm, and an emission maximum of 525 nm (A + C; Coble, 1996). Previous studies have found that fluorophores with a red-shifted Ex/Em maximum tend to be more aromatic, and have a greater molecular weight (Fellman et al., 2008; Cuss and Guéguen, 2012b). This component is similar to those representative of soil humic substances (Stedmon and Markager, 2005; Singh et al., 2010).

Component 3 (C3) was the only protein-like component observed, and had an excitation/emission maximum of 260/315 nm. This component was subsequently labelled as a tyrosine-like peak (peak B; Coble, 1996). Components similar to C3 have also been observed in DOM found in leaf leachate (Cuss and Guéguen, 2013), and are often associated with biological activity in natural waters (Coble, 1996; Stedmon and Markager, 2005). A similar protein-like peak was also observed in biochar extracts, and was especially prevalent in biochars made from lignin-rich feedstocks (Uchimiya et al., 2013). Protein-like fluorescence has been correlated with the biodegradable fraction of DOC (Fellman et al., 2008; Cuss and Guéguen, 2012a).

To examine transformations of biochar-derived DOM over time, component loadings and percent composition were compared using measurements taken at the beginning and end of the leaching experiment (i.e. day 3 and day 17, respectively; Fig. 4). PARAFAC loadings were normalized by dividing by the respective DOC concentrations measured in each sample. Thus, normalized

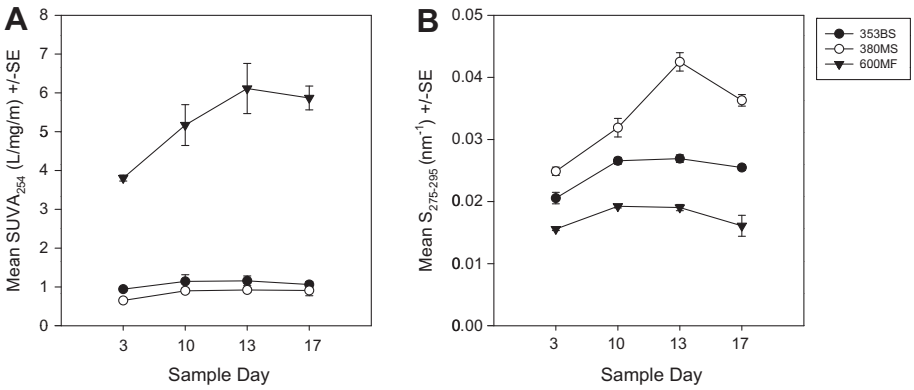

Fig. 2. Mean SUVA254 (A) and $S_{275-295}$ (B) measurements observed over the course of leaching experiment. Error bars indicate standard error.

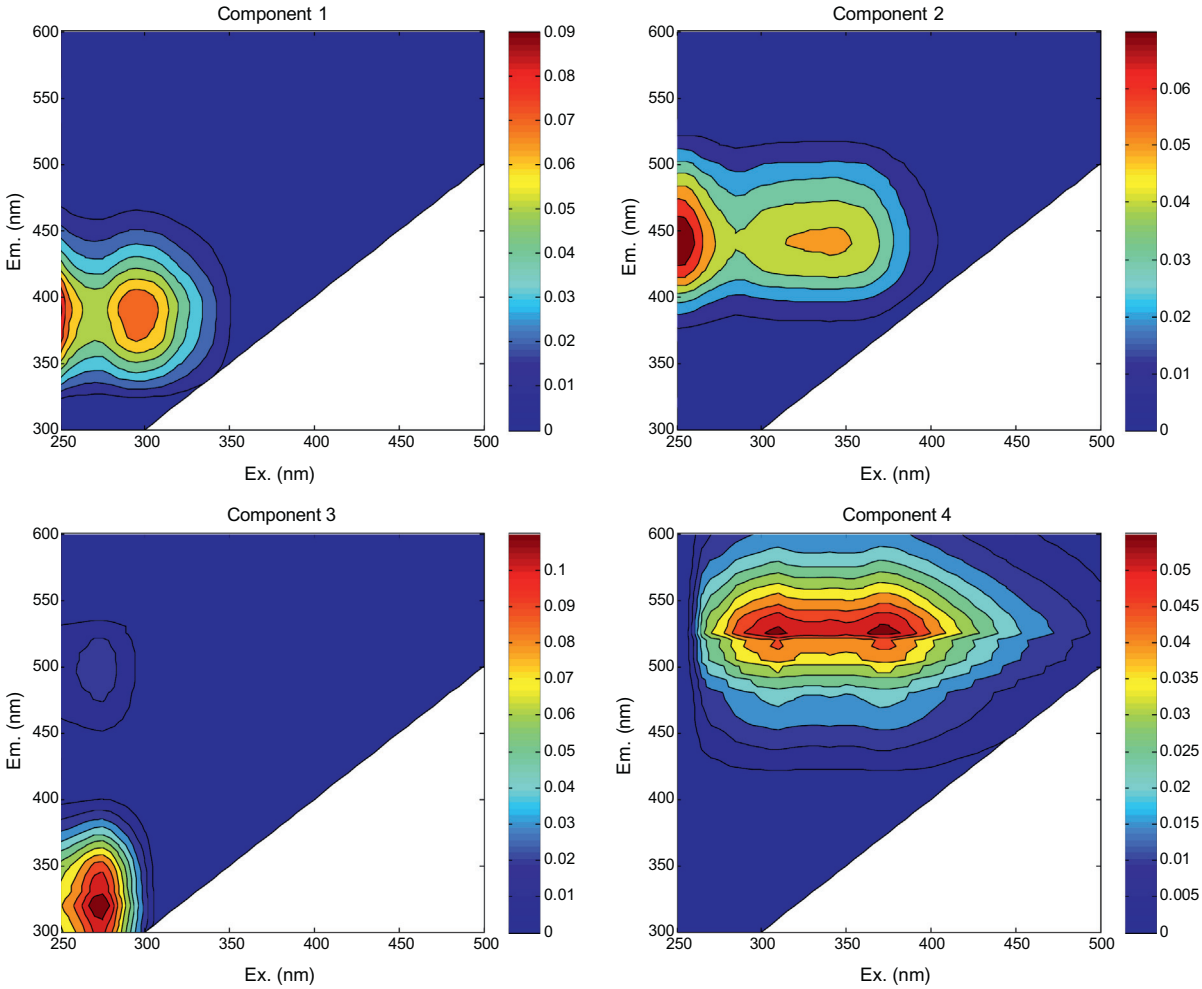

Fig. 3. Contour plots of PARAFAC components.

loadings represent fluorescence intensity representative of the quantum yield of each fluorophore. After 3 d of leaching, DOM derived from 600MF showed the highest fluorescence intensity per unit of DOC, followed by 353BS, and 380MS (Fig. 4A). On day 3, the dominant component was biochar-dependent; low temperature biochars (i.e. 353BS and 380MS) had similar mean C1 and C3 loadings (0.04 and 0.04 for 353BS; and 0.03 and 0.02 for 380MS, respectively), while protein-like C3 was predominant in the high temperature biochar (600MF; 0.10) (Fig. 4A). The difference in component loadings for the same feedstock (600MF and 380MS) indicates a clear effect of pyrolytic conditions, suggesting that the increased furnace residence times used to produce 380MS resulted in a reduction in fluorescence intensity. Uchimiya et al. (2013) found that total fluorescence intensity in biochar-DOM generally decreased with increasing pyrolysis temperature, which is similar to the present observations. This further suggests that 600MF may be underpyrolyzed compared to 380MS. Compared to day 3 measurements, significant increases in component

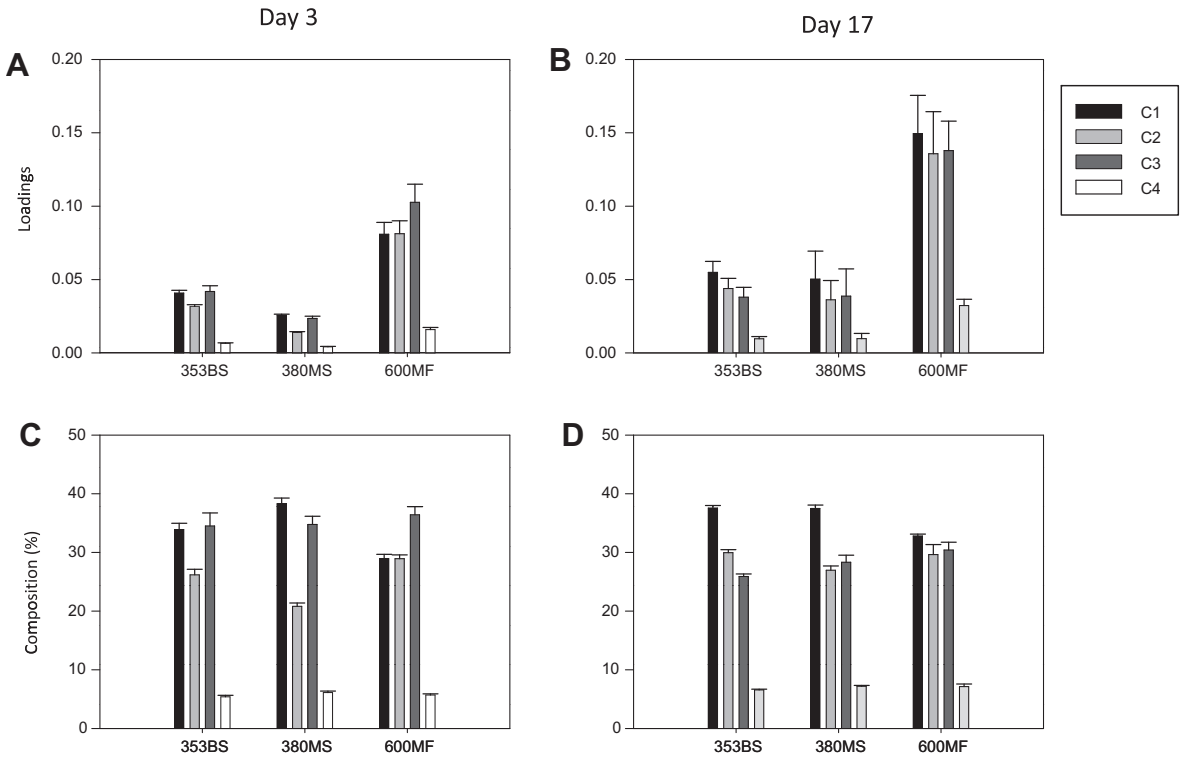

Fig. 4. PARAFAC component loadings measured on day 3 and 17 (A and B, respectively), and their proportional distribution (C and D, respectively). Error bars indicate standard error.

loadings were observed on day 17, suggesting an increase in fluorescing DOM concentration (Fig. 4B). All biochar leachates showed a significant increase in humic-like fluorescence (C1, C2, C4; $p < 0.05$), while only 600MF showed an increase in protein-like fluorescence (C3; $p < 0.05$), which could be the result of the lower furnace residence time used in its production. This indicates an increase in fluorescence intensity per unit of DOC over time, and thus a significant change in DOM quality.

Significant differences in the proportional distribution of the components were also observed (Fig. 4C and D). On day 3, the proportion of C1 was significantly different amongst all biochar types ($p < 0.01$; Fig. 4C), and followed the order 380MS > 353BS > 600MF. The proportion of C2 was significantly lower in 380MS leachate ($p < 0.0001$), but similar in 353BS and 600MF (Fig. 4C). The proportion of protein-like C3 was not significantly different amongst biochar types, but it was found to be the dominant component in 600MF leachate (Fig. 4C). This was similar to observations made by Uchimiya et al. (2013) who found this component to be thermally stable. The proportion of C4 was also found to be similar amongst all biochar types (Fig. 4C). It was noted that the proportions of C1 and C2 varied significantly in DOM from 600MF and 380MS, while C3 and C4 remained stable. In 600MF leachate, C1 and C2 were very similar in proportion, while in 380MS leachate, the proportion of C1 was higher, and the proportion of C2 was lower. This, taken into account with the lower component loadings observed in 380MS (Fig. 4A), suggests that pyrolysis not only affects the content of fluorescent material in biochar DOM, but also affects fluorophores to different degrees. This effect is also similar to observations made by Lin et al. (2012) and Uchimiya et al. (2013) who found a proportional shift in certain DOM fractions as an effect of pyrolysis temperature. Further, Cuss and Guéguen (2013) found the proportions of a protein-like component and a marine/microbial humic-like component to be dominant in unfractionated DOM leached from sugar maple (*A. saccharum*) leaves, which was similar to results observed in 600MF and 380MS. Compared to day 3, significant fluctuations in the proportional distribution of components on day 17 were also observed. An increase in the proportion of C1 loadings were significant only in 600MF ($p < 0.05$; Fig. 4D). The percentage of C2 showed a significant increase in only 353BS and 380MS ($p < 0.01$; Fig. 4D). All biochars showed a significant increase in the proportion of C4 ($p < 0.05$), but a decrease in the proportion of C3 ($p < 0.05$). Clear differences in the behaviour of DOM were observed in biochars made from the same feedstock under different pyrolytic conditions (600MF and 380MS).

3.4. Principal component analysis

The ordination of the first two principal components (PC1 and PC2; 48.6% and 28.9% variance, respectively) explained 77.4% of total variance (Fig. 5). Positive loadings in PC1 were found for $SUVA_{254}$ and humic-like C2 and protein-like C3 whereas negative loadings were associated with $S_{275-295}$, humic-like C1 and C4, and it can be said that PC1 represents the aromaticity of the biochar-derived DOM. On the other hand, PC2 represents the change in fluorescence composition with positive loadings associated with protein-like C3 and negative loadings with humic-like C2 and C4. A clear separation in scores was observed based on biochar type (Fig. 5), confirming significant differences in WSOC characteristics. PC1 and PC2 were found to be significantly correlated for all biochar types ($r^2 = 0.73$, $r^2 = 0.78$, $\rho = 0.82$ for 353BS, 380MS, and 600MF, respectively; Fig. 5). This is likely an effect of time, as PC1 and PC2 scores were significantly negatively correlated with leaching time for all biochar types ($p < 0.01$), except for 380MS, which showed no significant correlation between PC1 scores and time ($r^2 = -0.44$, $p = 0.07$). In general, the observed pattern confirms a shift in the proportions of protein-like components (C3) and humic-like components (C1, C2, C4) over time. This could be from an increase in the proportion of humic-like fluorescence, a

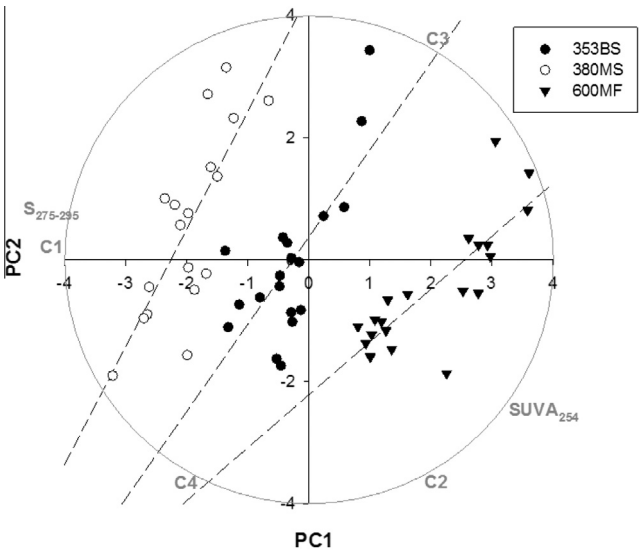

Fig. 5. PCA ordination with correlation circle for mean proportional PARAFAC loadings, SUVA254, and $S_{275-295}$. Dashed lines indicate a significant correlation between PC1 and PC2 ($r^2 = 0.73$, $r^2 = 0.78$, $\rho = 0.82$ for 353BS, 380MS, and 600MF, respectively).

decline in proportion of protein-like fluorescence, or a combination of these effects. In a previous study, Cuss and Guéguen (2012a) observed a decrease in the proportion of protein-like components observed in sugar maple leaf leachate, after inoculating samples with microbes. This, taken into consideration with previous observations, further supports the possibility of microbial activity in the biochar leachates. Previous studies have suggested that some biochars may provide a bioavailable source of carbon for soil microbes (Deenik et al., 2010; Bruun et al., 2012). Although our results do not allow us to conclusively state that microbial activity is responsible for the observed transformations in the fluorescence properties of biochar DOM, it does show that EEM fluorescence spectroscopy and PARAFAC can provide valuable insight into the qualities of biochar DOM, and allow for the observation of transformations in those qualities over time.

4. Conclusion

Biochar is growing in popularity in various environmental applications, but the feasibility of its use is directly dependent on its various physical and chemical properties. This includes the characteristics of biochar-derived DOM. The goal of this study was to assess the use of UV–visible absorption and EEM-fluorescence spectroscopy for the purpose of characterizing biochar-derived DOM. The results showed that the biochar produced at high temperatures with a lower furnace residence time (600MF) had a greater WSOC content than those produced at lower temperatures with longer residence times (353BS and 380MS). The UV–visible absorption results indicate that DOM derived from 600MF had a greater aromaticity and mean molecular weight than both 353BS and 380MS. Results from EEM-fluorescence and PARAFAC showed that 600MF had a greater fluorophore content per unit of DOC than both 353BS and 380MS, and significant increases in fluorescence intensity per unit of DOC were observed over time. Significant differences were also observed in the proportional distribution of PARAFAC components, which could be attributed to differences in feedstocks and pyrolytic conditions. The proportional distribution was observed to change over time, which could be the result of transformations in the qualitative characteristics of biochar-derived DOM over time. This study underscores the need for further studies into the characteristics in biochar-derived DOM, as well as its behaviour in natural environments.

Acknowledgements

The authors thank A. Perroud for DOC analysis. The authors would also like to acknowledge J. Balch, P. Dainard, C. Cuss and two anonymous reviewers for helpful comments and suggestions that helped improve the quality of this manuscript. This work was funded in part by the Canada Research Chairs program and the Canadian National Science and Engineering Research Council.

Appendix A. Supplementary material

Supplementary data associated with this article can be found, in the online version, at http://dx.doi.org/10.1016/j.chemosphere.2013.11.066.

References

Andrade-Eiroa, Á., Canle, M., Cerdá, V., 2013. Environmental application of excitation–emission spectrofluorimetry: an in-depth review I. Appl. Spectrosc. Rev. 48, 1–49.

Beesley, L., Moreno-Jiménez, E., Gomez-Eyles, J., 2010. Effects of biochar and greenwaste compost amendments on mobility, bioavailability and toxicity of inorganic and organic contaminants in a multi-element polluted soil. Environ. Pollut. 158, 2282–2287.

Beesley, L., Moreno-Jiménez, E., Gomez-Eyles, J., Harris, E., Robinson, B., Sizmur, T., 2011. A review of biochars' potential rolse in the remediation, revegetation and restoration of contaminated soils. Environ. Pollut. 159, 3269–3282.

Blough, J.E., Del Vecchio, R., 2002. Chromophoric DOM in the coastal environment. In: Hansel, D.A., Carlson, C.A. (Eds.), Biogeochemistry of Marine Dissolved Organic Matter. Associated Press, San Diego, pp. 509–546.

Bruun, E.Q., Ambus, P., Egsgaard, H., Hauggaard-Nielsen, H., 2012. Effects of slow and fast pyrolysis biochar on soil C and N turnover dynamics. Soil Biol. Biochem. 46, 73–79.

Carlson, C.A., 2002. Production and removal processes. In: Hansell, D.A., Carlson, C.A. (Eds.), Biogeochemistry of Marine Dissolved Organic Matter. Associated Press, San Diego, pp. 91–151.

Coble, P.G., 1996. Characterization of marine and terrestrial DOM in seawater using excitation–emission matrix spectroscopy. Mar. Chem. 51, 325–346.

Cuss, C.W., Guéguen, C., 2012a. Impacts of microbial activity on the optical and copper-binding properties of leaf-litter leachate. Front. Microbiol., 3. http://dx.doi.org/10.3389/fmicb.2012.0016.

Cuss, C.W., Guéguen, C., 2012b. Determination of relative molecular weights of fluorescent components in dissolved organic matter using asymmetrical flow field-flow fractionation and parallel factor analysis. Anal. Chim. Acta 733, 98–102.

Cuss, C.W., Guéguen, C., 2013. Distinguishing dissolved organic matter at its origin: size and optical properties of leaf-litter leachates. Chemosphere. http://dx.doi.org/10.1016/j.chemosphere.2013.03.06.

Deenik, J.L., McClellan, T., Uehara, G., Antal, M.J., Campbell, S., 2010. Charcoal volatile matter content influences plant growth and soil nitrogen transformations. Soil Sci. Soc. Am. J. 74 (4), 1259–1270.

Downie, A., Crosky, A., Munroe, P., 2009. Physical properties of biochar. In: Lehmann, J., Joseph, S. (Eds.), Biochar for Environmental Management: Science and Technology. Earthscan, London, pp. 13–32.

Fellman, J.B., D'Amore, D.V., Hood, E., Boone, R.D., 2008. Fluorescence characteristics and biodegradability of dissolved organic matter in forest and wetland soils from coastal temperate watersheds in southeast Alaska. Biogeochemistry 88, 169–184.

Gaskin, J.W., Steiner, C., Harris, K., Das, K.C., Bibens, B., 2008. Effect of low-temperature pyrolysis conditions on biochar for agricultural use. T. ASABE 51 (6), 2061–2069.

Guéguen, C., Cuss, C.W., 2011. Characterization of aquatic dissolved organic matter by asymmetrical flow field-flow fractionation coupled to UV–visible diode array and excitation emission matrix fluorescence. J. Chromotogr. A 1218, 4188–4198.

Guéguen, C., Gilbin, R., Pardos, M., Dominik, J., 2004. Water toxicity and metal contamination assessment of a polluted river: the Upper Vistula River (Poland). Appl. Geochem. 19, 153–162.

Guéguen, C., Burns, D.C., McDonald, A., Ring, B., 2012. Structural and optical characterization of dissolved organic matter from the lower Athabasca River, Canada. Chemosphere 87, 932–937.

Helms, J.R., Stubbins, A., Ritchie, J.D., Minor, E., Kieber, D.J., Mopper, K., 2008. Absorption spectral slope ratios as indicators of molecular weight, source, and photobleaching of chromophoric dissolved organic matter. Limnol. Oceanogr. 53 (3), 955–969.

Ishii, S.K., Boyer, T.H., 2012. Behavior of reoccurring PARAFAC components in fluorescent dissolved organic matter in natural and engineered systesm: a critical review. Environ. Sci. Technol. 46, 2006–2017.
Kalbitz, K., Solinger, S., Park, J.H., Michalzik, B., Matzner, E., 2000. Controls on the dynamics of dissolved organic matter in soils: a review. Soil Sci. 165, 277–304.
Kloss, S., Zehetner, F., Dellantonio, A., Hamid, R., Ottner, F., Liedtke, V., Schwanninger, M., Gerzabek, M.H., Soja, G., 2012. Characterization of slow pyrolysis biochars: effects of feedstocks and pyrolysis temperature on piochar properties. J. Environ. Qual. 41, 990–1000.
Lawaetz, A.J., Stedmon, C.A., 2009. Fluorescence intensity calibration using the Raman scatter peak of water. Appl. Spectrosc. 63 (8), 936–940.
Lin, Y., Munroe, P., Joseph, S., Henderson, R., Ziolkowski, A., 2012. Water extractable organic carbon in untreated and chemical treated biochars. Chemosphere 87, 151–157.
Maie, N., Scully, N.M., Pisani, O., Jaffé, R., 2007. Composition of a protein-like fluorophore of dissolved organic matter in coastal wetland and estuarine ecosystems. Water Res. 41 (3), 563–570.
Mukherjee, A., Zimmerman, A.R., 2013. Organic carbon and nutrient release from a range of laboratory-produced biochars and biochar-soil mixtures. Geoderma 193–194, 122–130.
Pawlosky-Glahn, V., Egozcue, J.J., 2006. Compositional data and their analysis: an introduction. Geol. Soc. London Spec. Publ. 264, 1–10.
Singh, S., D'Sa, E.J., Swenson, E.M., 2010. Chromophoric dissolved organic matter (CDOM) variability in Barataria Basin using excitation–emission matrix (EEM) fluorescence and parallel factor analysis (PARAFAC). Sci. Total Environ. 408, 3211–3222.
Spokas, K.A., Cantrell, K.B., Novak, J.M., Archer, D.W., Ippolito, J.A., Collins, H.P., Boateng, A.A., Lima, I.M., Lamb, M.C., McAloon, A.J., Lentz, R.D., Nichols, K.A., 2012. Biochar: a synthesis of its agronomic impact beyond carbon sequestration. J. Environ. Qual. 41, 973–989.
Stedmon, C.A., Bro, R., 2008. Characterizing dissolved organic matter fluorescence with parallel factor analysis: a tutorial. Limnol. Oceanogr. Methods 6, 572–579.
Stedmon, C.A., Markager, S., 2005. Resolving the variability in dissolved organic matter fluorescence in a temperature estuary and its catchment using PARAFAC analysis. Limnol. Oceanogr. 50 (2), 686–697.
Stedmon, C.A., Markager, S., Bro, R., 2003. Tracing dissolved organic matter in aquatic environments using a new approach to fluorescence spectroscopy. Mar. Chem. 82, 239–254.
Tipping, E., 2002. Cation Binding by Humic Substances. Cambridge University Press, Cambridge.
Uchimiya, M., Lima, I.M., Klasson, L.K., Wartelle, L.H., 2010. Contaminant immobilization and nutrient release by biochar soil amendment: roles of natural organic matter. Chemosphere 80, 935–940.
Uchimiya, M., Ohno, T., He, Z., 2013. Pyrolysis temperature-dependent release of dissolved organic carbon from plant, manure, and biorefinery Wastes. J. Anal. Appl. Pyrolysis. http://dx.doi.org/10.1016/j.jaap.2013.09.00.
Weishaar, J.L., Aiken, G.R., Bergamaschi, B.A., Fram, M.S., Fuji, R., Mopper, K., 2003. Evaluation of specific ultraviolet absorbance as an indicator of the chemical composition and reactivity of dissolved organic carbon. Environ. Sci. Technol. 37, 4702–4708.